

A Comprehensive Analysis of Parkinson's Disease Detection Through Inertial Signal Processing

Manuel Gil-Martín, Sergio Esteban-Romero, Fernando Fernández-Martínez
and Rubén San-Segundo

Grupo de Tecnología del Habla y Aprendizaje Automático (T.H.A.U. Group), Information Processing and Telecommunications Center, E.T.S.I. de Telecomunicación, Universidad Politécnica de Madrid, Madrid, Spain

Keywords: Parkinson's Disease Detection, Inertial Signals, Fast Fourier Transform, Tremor Detection, Convolutional Neural Networks, Window Size.

Abstract: When developing deep learning systems for Parkinson's Disease (PD) detection using inertial sensors, a comprehensive analysis of some key factors, including data distribution, signal processing domain, number of sensors, and analysis window size, is imperative to refine tremor detection methodologies. Leveraging the PD-BioStampRC21 dataset with accelerometer recordings, our state-of-the-art deep learning architecture extracts a PD biomarker. Applying Fast Fourier Transform (FFT) magnitude coefficients as a preprocessing step improves PD detection in Leave-One-Subject-Out Cross-Validation (LOSO CV), achieving 66.90% accuracy with a single sensor and 6.4-second windows, compared to 60.33% using raw samples. Integrating information from all five sensors boosts performance to 75.10%. Window size analysis shows that 3.2-second windows of FFT coefficients from all sensors outperform shorter or longer windows, with a window-level accuracy of 80.49% and a user-level accuracy of 93.55% in a LOSO scenario.

1 INTRODUCTION

Research on biometrics has experienced notable growth in recent years, witnessing a surge in various applications, particularly in the field of healthcare. The term healthcare biometrics is not only confined to biometric applications for controlling access to electronic medical records and patient identification but also includes medical decision support tools for patient care. These tools extract biomarkers that define patient health and aid in illness detection, medication response analysis, and the management of chronic conditions such as Parkinson's Disease (PD). PD is a neurodegenerative disorder characterized by motor impairments like tremor, bradykinesia, rigidity, and postural instability (Jankovic, 2008). These impairments affect various motor functions, including planning, programming, sequencing, movement initiation, and execution.

Deep learning algorithms have been applied on human motion recognition to model the evolution of physical activities using wearables or cameras (Manuel Gil-Martín, San-Segundo, Fernández-Martínez, & Ferreiros-Lopez, 2020, 2021; Gil-

Martín, San-Segundo, Fernández-Martínez, & de Córdoba, 2020; Zhang et al., 2017). This way, the tremor movement related to PD could be also model by these technologies.

This work proposes a PD detection system based on a deep learning architecture that allows analyzing different important aspects to consider when using tremor to distinguish between healthy people and PD patients. The primary contributions of this research are as follows:

- Analysis of the inertial signal domain for PD detection.
- Assessment of different sensors to detect PD.
- Study of the window length on PD detection.

This paper is organized as follows. Section 2 reviews the literature of PD detection using inertial sensors. Section 3 reviews the material and methods, including a description of the dataset, the signal processing, the deep neural network, and the evaluation methodology. Section 4 describes the experiments and the obtained results and section 5 summarizes the main conclusions of the paper.

2 RELATED WORKS

Many researchers have explored the use of machine learning to detect motor symptoms of Parkinson's disease using wearable sensors (Channa, Ifrim, Popescu, & Popescu, 2021; Iakovakis et al., 2020; Kubota, Chen, & Little, 2016). Some of these works address the simultaneous detection of multiple symptoms (Lang et al., 2019). Despite this significant interest, there are still several aspects that need improvement, such as overall accuracy in real-world settings, the acquisition of clinically significant metrics, and robust detection in patients for whom there is no training data.

Regarding the extraction of features from inertial signals, many feature sets have been proposed in the literature for Parkinson's disease detection based on tremor. The vast majority of these are based on measurements in the time domain (such as mean, range, or cross-correlation), in the frequency domain (such as dominant frequency, energy content in a particular band, or signal entropy) (Rigas et al., 2012), or a combination of the two (Dai, Zhang, & Lueth, 2015). Some authors have demonstrated that features traditionally used for speech processing (e.g., frequency analysis using the Mel scale, cepstral coefficients) are also effective in classifying human motion from accelerometer data (San-Segundo, Manuel Montero, Barra-Chicote, Fernandez, & Manuel Pardo, 2016; San-Segundo, Navarro-Hellin, Torres-Sanchez, Hodgins, & De la Torre, 2019; Vanrell, Milone, & Rufiner, 2018).

As for tremor classification or detection algorithms, researchers have experimented with a wide variety of machine learning algorithms, such as decision trees (Garcia-Magarino, Medrano, Plaza, & Oliván, 2016), random forests (Arora et al., 2015), hidden Markov models (Rigas et al., 2012), and neural networks (Cole, Roy, De Luca, Nawab, & Ieee, 2010). For example a previous work (Hathaliya et al., 2022) used a deep learning architecture to model tremor obtaining a 92.4% of accuracy using 6.4-second windows of raw samples using a single sensor on the left anterior forearm. However, the data distribution used in this work seems to simulate a too optimistic scenario since data from the same subjects were included in both training and testing subsets. In addition, there exists a lack of a deep study of window sizes to select the most appropriate one to predict the tremor.

This work proposes the use of a deep network for both feature learning and tremor detection in a realistic scenario and deeply analyse different aspects that could affect the final performance, such

as the data distribution, the input signal domain, the sensors used to feed the system and the size of the analysis windows. Some of these aspects have been analysed in activity recognition (Gil-Martín et al., 2020) but not in PD detection.

3 MATERIALS AND METHODS

This section describes the dataset, the signal processing, the deep neural network used for the PD detection and the followed evaluation methodology.

3.1 Dataset

The PD-BioStampRC21 dataset (Adams et al., 2021) includes tri-axial accelerometer obtained from five wearable sensors, involving both PD and healthy control participants. Lightweight MC 10 BioStamp RC sensors were used to collect the data, with each participant wearing five sensors attached to specific body parts, including the chest, left anterior thigh, right anterior thigh, left anterior forearm, and right anterior forearm as observed in Figure 1. The samples were obtained at a sampling rate of 31.25 Hz. Moreover, the dataset contains information about the participants' medication status and the Unified Parkinson's Disease Rating Scale (UPDRS) but they were not used in this work. The dataset contains recordings from 34 subjects: 17 healthy control and 17 PD participants. However, after analysing the available dataset, it was found that some sensors from control participants with IDs 007, 014, and 060 had missing data, so they were removed from the study.

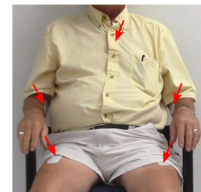


Figure 1: A study participant wearing the sensors at five different locations on the chest and each limb (Adams et al., 2021).

3.2 Signal Processing

In this work, two input formats of the inertial signals were evaluated to feed a deep neural network: Raw data and Fast Fourier Transform (FFT) magnitude coefficients. As in the baseline system (Hathaliya et al., 2022) we used 30,000 readings (16.13 minutes) for each participant along with their status in order

to feed the classification system and analyse the effect of particular aspects instead of using the whole dataset (Igene, Alim, Intiaz, & Schuckers, 2023).

First, we divided the recordings into overlapped windows (a shift equivalent to half the window size between consecutive windows). The system classifies each window to healthy control or PD. All the windows from each participant were labelled as healthy control or PD depending on the participant's health status. In this work, we evaluated the classification performance when considering different window sizes of 0.8, 1.6, 3.2, 6.4, 12.8 and 16 seconds corresponding to 25, 50, 100, 200, 300 and 400 time samples, respectively.

Second, for each window size, we analysed both time and frequency domain signals as inputs to a deep neural network, considering two different preprocessing steps depending on the signal domain. In the first case, no preprocessing was done to the original signal and the inputs to the deep neural network were directly the time samples included in each window (Raw data). In the second case, the inputs were the coefficients of the FFT magnitude. These coefficients were precomputed for each analysis window and represented the spectrum from 0 Hz to half of the sampling frequency, 15.625 Hz for the PD-BioStampRC21 dataset. As the energy in tremor motion mostly concentrates in low frequencies (M. Gil-Martin, Montero, & San-Segundo, 2019), the obtained spectrogram could be useful for the PD detection. This paper analyses and compares both alternatives for the tremor modelling.

3.3 Deep Learning Architecture

The deep learning architecture used in this work was a state-of-the-art Convolutional Neural Network (CNN) composed of two main parts: a feature learning subnet and a classification subnet. The first subnet learnt features from the raw data or FFT magnitude coefficients from the inertial signals using two convolutional layers (32 kernels of (1, 5) dimensions) and two max-pooling layers (kernels of (1, 2) dimensions). The second subnet used fully connected layers to classify the learned features as a predicted class: healthy person (0) or PD patient (1). The architecture included dropout layers (0.3) after max-pooling and fully connected layers to avoid overfitting during training. The last layer used a SoftMax activation function to offer the predictions of each class for every analysis frame, while intermediate layers used ReLU for reducing the

impact of gradient vanishing effect. We used categorical cross-entropy as loss metric and the Adaptive Moment Estimation (Adam) optimizer, which adaptively adjusts the learning rate throughout training. We adjusted the epochs and batch size of the deep learning structure to 30 and 100, respectively. Figure 2 represents the architecture used in this work to model and classify the analysis windows to healthy person or PD patient. This architecture was implemented using the Keras library and Python programming language.

As observed in the figure, the inputs of the CNN were organized in a 2D matrix with $N \times M$ dimensions. N corresponds to the number of input signals: 3 when using a single sensor (X, Y and Z signals) or 15 when using the five available sensors in the dataset (3 x 5). M is the number of analyzed samples from each sensor signal. This number depends on the size of the analysis window and the signal domain used in each experiment. M is equal to the size of the analysis window when using raw data as input data. Nevertheless, in the frequency domain, M is the number of FFT coefficients obtained from each window, and it is equal to the half of the window size.

3.4 Evaluation Methodology

In this work, different data distributions have been used to compare to a baseline system and highlight the importance of correctly train and test a PD detection system.

The first data distribution, called TrainTest, consists of using an 80% of data for training and 20% of data for testing. This data distribution was used by the baseline system (Hathaliya et al., 2022). When randomly distribute overlapped windows, it is possible to train and test the system with examples that share information, which leads to a very optimistic performance. In addition, examples from the same subjects can be used for training and testing. However, one of the main problems of this data distribution is that the system is only evaluated over a particular subset of the whole dataset.

To evaluate the system using the whole dataset, it is possible to create a Cross-Validation (CV) alternative for this data distribution: TrainTest_CV. In this K-fold CV methodology, the given data are divided into k groups or folds to train and test a system with different data. This process is repeated changing the training and testing folds and the results are the average of the partial results obtained for all repetitions.

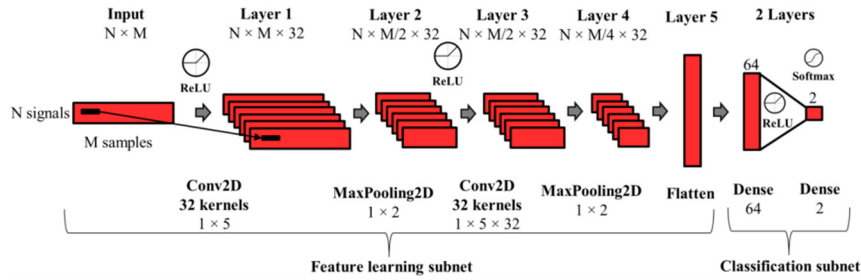


Figure 2: Convolutional Neural Network Architecture used in this work for PD detection where N denotes the number of input signals and M denotes the number of samples for each analysis window or example.

However, to avoid recordings from the same subjects in both training and testing subsets (a more realistic scenario), we decided to consider a Leave-One-Subject-Out (LOSO) CV, which is a specific type of K-fold CV where the system is evaluated with the data from one subject and is trained with the data from the rest of the subjects. In this case, the process is repeated several times leaving a different subject for testing and the results are also the average of the partial results obtained for all repetitions. This methodology simulates a more difficult and realistic scenario where the system is evaluated with recordings from subjects different to those used for training. Figure 3 shows examples for the data distributions described above.

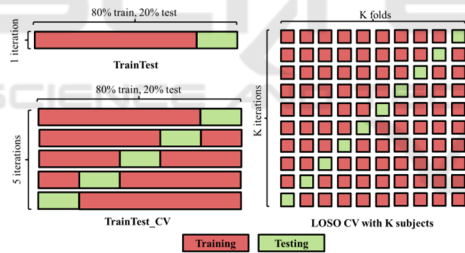


Figure 3: Data distributions for TrainTest, TrainTest_CV and LOSO CV methodologies.

As evaluation metrics, we used accuracy, which is defined as the ratio between the number of correctly classified samples and the number of total samples. This way, for a classification problem with N testing examples and C classes, accuracy is defined in Equation (1).

$$\text{Accuracy} = \frac{1}{N} \sum_{i=1}^C P_{ii} \quad (1)$$

Considering R_i as the sum of all examples in a column of the confusion matrix, and S_i as the sum of all examples in a row, precision (Equation (2)), recall (Equation (3)) and F1score (Equation (4)) metrics are defined as follows:

$$\text{precision} = \frac{1}{C} \sum_{i=1}^C \frac{P_{ii}}{R_i} \quad (2)$$

$$\text{recall} = \frac{1}{C} \sum_{i=1}^C \frac{P_{ii}}{S_i} \quad (3)$$

$$\text{F1score} = 2 \cdot \frac{\text{precision} \cdot \text{recall}}{\text{precision} + \text{recall}} \quad (4)$$

To show statistical significance values, we used confidence intervals, which include plausible values for a specific metric. We will assure that there exists a significant difference between results of two experiments when their confidence intervals do not overlap. Equation (5) represents the computation of confidence intervals attached to a specific metric value and N samples for 95% confidence level.

$$\text{CI}(95\%) = \pm 1.96 \sqrt{\frac{\text{metric} \cdot (100 - \text{metric})}{N}} \quad (5)$$

In this work, we modelled the tremor at window-level since the examples used to feed the deep neural architecture were windows. However, we also provided a performance at user-level, considering the mode of the predictions for all the windows from a subject as the user prediction. This way, it is possible to integrate the information from all the windows in a single prediction, which is useful from a comprehensive medical perspective. This approach provides overall health trends instead of focusing exclusively on the presence or absence of tremors during brief time intervals that could potentially lead to incomplete or incorrect assessments.

4 RESULTS AND DISCUSSION

This section contains details about the experiments performed in this work, including results and discussion about the data distribution, the signal

domain, the sensors used to feed the system and the window size of the examples.

4.1 Data Distribution

The first experiments that we performed consists of using only the three signals from the left anterior forearm and a window size of 6.4 seconds (200 samples) in order to compare to the baseline system (Hathaliya et al., 2022). This previous work only states that they split the dataset into training (80%) and test (20%). They did not specify any aspect of considering the subject distributions to avoid mixing data from the same subject in training and testing subsets and did not mention any CV approach. This data distribution (TrainTest) leads to a very optimistic scenario where the system is trained and tested with examples from the same subjects that could share information since the windows are overlapped. This previous work obtained a 92.4% of accuracy. Simulating this scenario setup, our proposed system could easily reach the maximum performance (100% of accuracy) because the isolated experiment results would depend on the final testing examples. In order to obtain a more general performance evaluating the whole dataset, a CV approach of this scenario (TrainTest_CV) obtained 72.42 ± 0.91 % test accuracy.

Despite of this experiment, we considered a more realistic approach through a LOSO CV. With this scenario, the system obtained a test accuracy of 60.33 ± 1.0 %.

Table 1 summarizes the results for the different CV data distributions using Raw data 6.4-second windows. These approaches evaluated the same number of examples but simulate very different scenarios, where LOSO CV approach is a more realistic scenario because data from testing subjects were not included in the training process. For this reason, the performance of the LOSO CV approach decreased compared to the rest experiments.

To simulate a more realistic scenario, we decided to keep the LOSO CV approach for the rest of experiments of this study.

4.2 Signal Domain Analysis

Regarding the signal domain of the inputs, we decided to compare Raw data windows against using the FFT magnitude coefficients. Figure 4 shows a comparison of performance at window-level when using Raw data (60.33 ± 1.0 %) and FFT data (66.90 ± 0.96 %) of 6.4-second windows and left anterior forearm sensor. We observed a significant increment

of performance when using signals in the frequency domain.

Table 1: Evaluation metrics for different CV data distributions using Raw data 6.4-second windows and left anterior forearm sensor.

| Data distribution | Test Accuracy (%) | Test F1-score (%) |
|------------------------------------|-------------------|-------------------|
| TrainTest (Hathaliya et al., 2022) | 92.40 | - |
| TrainTest | 100.00 | 100.00 |
| TrainTest CV | 72.42 ± 0.91 | 71.56 ± 0.92 |
| LOSO CV | 60.33 ± 1.00 | 59.20 ± 1.00 |

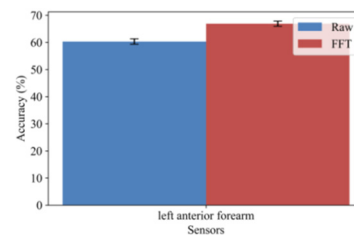


Figure 4: Accuracy at window-level using 6.4-second windows and left anterior forearm sensor depending on the input signal domain.

One of the possible reasons of this increment could be that PD tremor becomes more visible in the frequency domain: information of energy corresponding to the tremor frequency (between 3–9 Hz (Deuschl, Fietzek, Klebe, & Volkmann, 2003; M. Gil-Martin et al., 2019)) and its harmonics can be seen in the spectrum of the X, Y and Z signals of the inertial sensor. This way, the use of a CNN with FFT magnitude coefficients as inputs allowed obtaining better results compared to using raw data samples directly.

4.3 Sensors Analysis

Since the available dataset provides information from several sensors distributed over different locations in the body, we decided to analyse which sensor provide more valuable information regarding the tremor motion and combine the information from all of them. Figure 5 shows the accuracy at window-level using 6.4-second windows depending on the input signal domain (Raw or FFT) and sensors used to feed the deep learning architecture.

It is possible to observe that for all the systems (using a single sensor or all sensors together), using the FFT approach provides a significant improvement compared to directly using the raw samples. In addition, we observed that the systems

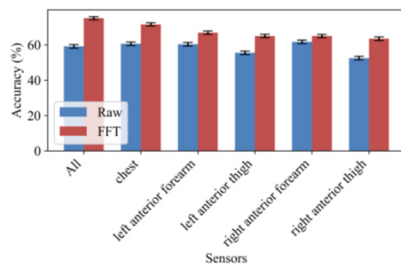


Figure 5: Accuracy at window-level using 6.4-second windows depending on the input signal domain and sensors.

using only the chest, left anterior forearm and or right anterior forearm sensors and the system using all the sensors together offer similar performance when using raw data (e.g., 60.60 ± 0.99 % test accuracy with the chest sensor). This means that the motion symptoms are more noticeable in the chest and upper limbs. Moreover, when analysing the FFT signal experiments, it is possible to observe that the chest is the single sensor that offers better performance (71.57 ± 0.92 %). However, using all the sensors provides a significant improvement compared to the rest of experiments (75.10 ± 0.88 %). Then, the CNN architecture is capable to integrate the information from the different sensors and learn more meaningful features to model the tremor.

For these reasons, we decided to use all the sensors for the rest of experiments of this study.

4.4 Window Size Analysis

To study the effect of the window size over the PD detection, we used windows of 0.8, 1.6, 3.2, 6.4, 12.8 and 16 seconds in time and frequency domain. As observed in Figure 6 and Figure 7, the binary classification performance showed improvement with an increase in the duration of the analysis window from 0.8 seconds to 3.2 seconds. However, it decreased after 3.2 seconds. When using long windows in a PD detection system that relies on deep learning algorithms, the performance tends to either saturate or decline. This occurrence could be explained based on two factors (Manuel Gil-Martin et al., 2021). Firstly, the increase in the window size raises the number of parameters that require training in the deep learning architecture. This aspect could affect the final performance, especially when the dataset has a limited number of examples for training. Secondly, long windows raise the risk of overfitting. For example, the application of the FFT on lengthy windows increments the frequency resolution, leading each hertz to be represented with

a larger number of data points. This resolution escalates the vulnerability to overfitting and undermines the robustness in a LOSO CV scenario. Consequently, generalizing the trained model for the evaluation of data from unseen subjects becomes challenging. In addition to these two factors, in the PD detection case study it is important to select an appropriate window size because long windows could mix tremor events with motion not associated to PD. When increasing the window size, the analysis windows could include most motion without PD glimpses. This could disturb the modelling process because the long windows could smooth the tremor peak and they could be classified as control. Moreover, as observed before for the 6.4-second windows analysis, the deep study through different window size confirms that the FFT coefficients provide significant higher performance compared to the Raw data for all the windows at window-level (Figure 6). Regarding, user-level classification (Figure 7), since LOSO methodology reduces the number of examples to the number of users, the confidence intervals are higher in this case, but there still exists a tendency of the improvement provided by the FFT. Even in this

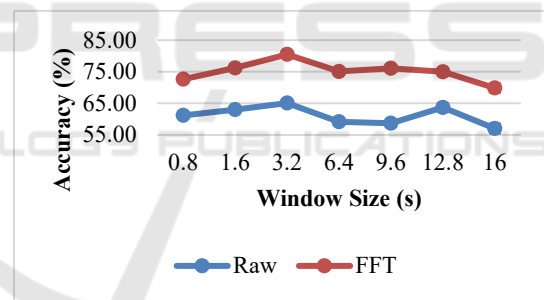


Figure 6: Window-level PD classification accuracy using all sensors depending on the window size and input signal domain.

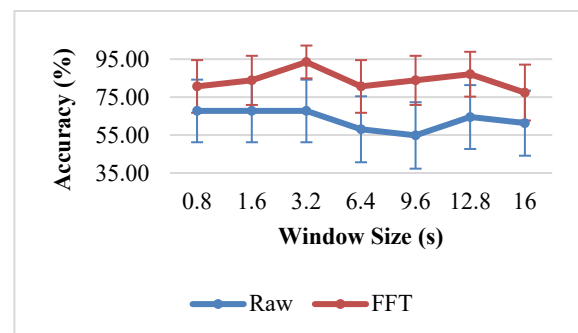


Figure 7: User-level PD classification accuracy using all sensors depending on the window size and input signal domain.

case, we observed that for 3.2-second windows, there exist significant difference between using Raw data and FFT. This FFT approach using windows of 3.2 seconds from all sensors reaches a window-level accuracy of 80.49 ± 0.57 % and a user-level accuracy of 93.55 ± 8.65 % in a LOSO scenario.

5 CONCLUSIONS

A comprehensive analysis is required when developing a deep learning system focused on PD detection using inertial sensors in order to highlight key factors to the refinement of tremor detection. This work uses the PD-BioStampRC21 dataset including healthy control and PD participants wearing five inertial sensors to perform a comprehensive study.

Ensuring an appropriate distribution of data is crucial in PD detection to prevent data overlap between training and testing subsets. The LOSO CV technique emerges as a robust solution, effectively mitigating the risk of data contamination and enhancing the model generalizability.

The use of FFT magnitude coefficients, in contrast to raw data samples, become helpful in detecting PD, particularly due to the pronounced visibility of tremor characteristics in the frequency domain. We obtained a significant improvement of performance when using FFT data (66.90 ± 0.96 %) of 6.4-second windows and left anterior forearm sensor compared to using directly Raw data (60.33 ± 1.0 %).

Incorporating multiple sensors located on the chest and limbs in CNN architecture capable of combining data exhibits the potential to increment the overall PD detection performance (75.10 ± 0.88 % when using FFT 6.4-second windows).

An in-depth exploration of the optimal analysis window size is imperative in enhancing the performance of both window-level and user-level evaluations. We observed that using 3.2-second analysis windows provides a positive balance between capturing intricate temporal patterns and preventing mixing tremor events with motion not associated to PD. This window size provided a window-level accuracy of 80.49 ± 0.57 % and a user-level accuracy of 93.55 ± 8.65 % in a LOSO scenario using the frequency domain of the input signals from all the sensors available in the dataset.

As future work, it would be possible to refine the data analysis. Specifically, the selection of windows with higher energy levels could aid in identifying instances when tremors are more pronounced,

thereby improving the performance of PD detection. In addition, the development of a robust regression system capable of accurately estimating UPDRS scores could offer valuable insights into disease progression and facilitate more precise monitoring of patients' motor symptoms. Moreover, it could be possible to investigate the optimal duration for data collection, beyond the current 16.13 minutes used in this work, and study the effect of the posture while collecting tremor data. Integrating these advancements into the proposed system holds substantial promise in advancing the field and contributing to the development of more effective diagnostic and monitoring tools for PD.

ACKNOWLEDGEMENTS

The work was supported by the project “TremorDetect - Detección de la enfermedad de Parkinson a través de señales inerciales”, funded by “Primeros Proyectos” call from ETSIT, UPM, by projects AMIC-PoC (PDC2021-120846-C42), GOMINOLA (PID2020-118112RB-C21 and PID2020-118112RB-C22) and BeWord (PID2021-126061OB-C43), supported by the Spanish Ministry of Science and Innovation (MCIN/AEI/10.13039/501100011033) and by the European Union “NextGenerationEU/PRTR”, and ASTOUND (101071191 HORIZON-EIC-2021-PATHFINDERCHALLENGES-01) funded by the European Commission.

REFERENCES

- Adams, J. L., Dinesh, K., Snyder, C. W., Xiong, M., Tarolli, C. G., Sharma, S., . . . Sharma, G. (2021). A real-world study of wearable sensors in Parkinson's disease. *npj Parkinson's Disease*, 7(1), 106. doi:10.1038/s41531-021-00248-w
- Arora, S., Venkataraman, V., Zhan, A., Donohue, S., Biglan, K. M., Dorsey, E. R., & Little, M. A. (2015). Detecting and monitoring the symptoms of Parkinson's disease using smartphones: A pilot study. *Parkinsonism & Related Disorders*, 21(6), 650-653. doi:10.1016/j.parkreldis.2015.02.026
- Channa, A., Ifrim, R.-C., Popescu, D., & Popescu, N. (2021). A-WEAR Bracelet for Detection of Hand Tremor and Bradykinesia in Parkinson's Patients. *Sensors*, 21(3). doi:10.3390/s21030981
- Cole, B. T., Roy, S. H., De Luca, C. J., Nawab, S. H., & Ieee. (2010, 2010 Aug 30-Sep 04). *Dynamic Neural Network Detection of Tremor and Dyskinesia from Wearable Sensor Data*. Paper presented at the 32nd Annual International Conference of the IEEE Engineering-in-Medicine-and-Biology-Society (EMBC 10), Buenos Aires, ARGENTINA.

- Dai, H., Zhang, P., & Lueth, T. C. (2015). Quantitative Assessment of Parkinsonian Tremor Based on an Inertial Measurement Unit. *Sensors*, 15(10), 25055-25071. doi:10.3390/s151025055
- Deuschl, G., Fietzek, U., Klebe, S., & Volkmann, J. (2003). Chapter 24 Clinical neurophysiology and pathophysiology of Parkinsonian tremor. In M. Hallett (Ed.), *Handbook of Clinical Neurophysiology* (Vol. 1, pp. 377-396): Elsevier.
- Garcia-Magarino, I., Medrano, C., Plaza, I., & Olivan, B. (2016). A smartphone-based system for detecting hand tremors in unconstrained environments. *Personal and Ubiquitous Computing*, 20(6), 959-971. doi:10.1007/s00779-016-0956-2
- Gil-Martin, M., Montero, J. M., & San-Segundo, R. (2019). Parkinson's Disease Detection from Drawing Movements Using Convolutional Neural Networks. *Electronics*, 8(8), 10. doi:10.3390/electronics8080907
- Gil-Martin, M., San-Segundo, R., Fernandez-Martinez, F., & Ferreiros-Lopez, J. (2020). Improving physical activity recognition using a new deep learning architecture and post-processing techniques. *Engineering Applications of Artificial Intelligence*, 92. doi:10.1016/j.engappai.2020.103679
- Gil-Martin, M., San-Segundo, R., Fernandez-Martinez, F., & Ferreiros-Lopez, J. (2021). Time Analysis in Human Activity Recognition. *Neural Processing Letters*. doi:10.1007/s11063-021-10611-w
- Gil-Martin, M., San-Segundo, R., Fernández-Martínez, F., & de Córdoba, R. (2020). Human activity recognition adapted to the type of movement. *Computers & Electrical Engineering*, 88, 106822. doi:https://doi.org/10.1016/j.compeleceng.2020.106822
- Hathaliya, J. J., Modi, H., Gupta, R., Tanwar, S., Sharma, P., & Sharma, R. (2022). Parkinson and essential tremor classification to identify the patient's risk based on tremor severity. *Computers & Electrical Engineering*, 101. doi:10.1016/j.compeleceng.2022.107946
- Iakovakis, D., Mastoras, R. E., Hadjidimitriou, S., Charisis, V., Bostanjopoulou, S., Katsarou, Z., . . . Ieee. (2020, 2020 Jul 20-24). *Smartwatch-based Activity Analysis During Sleep for Early Parkinson's Disease Detection*. Paper presented at the 42nd Annual International Conference of the IEEE-Engineering-in-Medicine-and-Biology-Society (EMBC), Montreal, CANADA.
- Igene, L., Alim, A., Imtiaz, M. H., & Schuckers, S. (2023). A Machine Learning Model for Early Prediction of Parkinson's Disease from Wearable Sensors. *2023 IEEE 13th Annual Computing and Communication Workshop and Conference, Ccwc*, 734-737. doi:10.1109/ccwc57344.2023.10099230
- Jankovic, J. (2008). Parkinson's disease: clinical features and diagnosis. *Journal of Neurology, Neurosurgery & Psychiatry*, 79(4), 368-376. doi:10.1136/jnnp.2007.131045
- Kubota, K. J., Chen, J. A., & Little, M. A. (2016). Machine learning for large-scale wearable sensor data in Parkinson's disease: Concepts, promises, pitfalls, and futures. *Movement Disorders*, 31(9), 1314-1326. doi:10.1002/mds.26693
- Lang, M., Pfister, F. M. J., Frohner, J., Abedinpour, K., Pichler, D., Fietzek, U., . . . Hirche, S. (2019). A Multi-Layer Gaussian Process for Motor Symptom Estimation in People With Parkinson's Disease. *Ieee Transactions on Biomedical Engineering*, 66(11), 3038-3049. doi:10.1109/tbme.2019.2900002
- Rigas, G., Tzallas, A. T., Tsipouras, M. G., Bougia, P., Tripoliti, E. E., Baga, D., . . . Konitsiotis, S. (2012). Assessment of Tremor Activity in the Parkinson's Disease Using a Set of Wearable Sensors. *Ieee Transactions on Information Technology in Biomedicine*, 16(3), 478-487. doi:10.1109/titb.2011.2182616
- San-Segundo, R., Manuel Montero, J., Barra-Chicote, R., Fernandez, F., & Manuel Pardo, J. (2016). Feature extraction from smartphone inertial signals for human activity segmentation. *Signal Processing*, 120, 359-372. doi:10.1016/j.sigpro.2015.09.029
- San-Segundo, R., Navarro-Hellin, H., Torres-Sanchez, R., Hodgins, J., & De la Torre, F. (2019). Increasing Robustness in the Detection of Freezing of Gait in Parkinson's Disease. *Electronics*, 8(2). doi:10.3390/electronics8020119
- Vanrell, S. R., Milone, D. H., & Rufiner, H. L. (2018). Assessment of Homomorphic Analysis for Human Activity Recognition From Acceleration Signals. *Ieee Journal of Biomedical and Health Informatics*, 22(4), 1001-1010. doi:10.1109/jbhi.2017.2722870
- Zhang, S., Wei, Z., Nie, J., Huang, L., Wang, S., & Li, Z. (2017). A Review on Human Activity Recognition Using Vision-Based Method. *Journal of Healthcare Engineering*, 2017. doi:10.1155/2017/3090343.